Mineralogia, vol. 54, 2023, 11-17 *Letter*

DOI: 10.2478/mipo-2023-0002

Britholite-(Ce) from the metaluminous granite of SW Egypt

Kamaleldin M. Hassan*

Nuclear Materials Authority, El Katameya, New Cairo 3, Cairo Governorate 4710030, Egypt

*Corresponding author: egy100@yahoo.com

Abstract

Optical microscopy and scanning electron microscopy-energy dispersive X-ray spectroscopy (SEM-EDS) analyses were used to characterize britholite-(Ce) of the metaluminous granite (Proterozoic) intruded into the Nubian Formation in southwestern Egypt and having a relatively high content of radioactive elements (potassium = 4.4 wt%, thorium = 52 ppm, uranium = 10 ppm). The britholite-(Ce) studied here incorporates light rare earth elements (LREE) including lanthanum, cerium, praseodymium, and neodymium as well as thorium. The mineral forms as tabular crystals in a fine-grained quartz-K-feldspar-plagioclase matrix, coexisting with other accessory minerals including biotite, zircon, clinochlore, titanite, and magnetite. Primary britholite-(Ce) usually includes titanite, zircon, and magnetite and is occasionally included in biotite. The inclusion of britholite-(Ce) in biotite suggests that the two minerals crystallized approximately coevally. Petrographical and SEM-EDS data indicate breakdown of the primary magmatic britholite-(Ce) in the samples. This study constitutes the first report for a sole presence of britholite-(Ce) as LREE phase in metaluminous granite samples from Egypt.

Keywords: Britholite-(Ce), metaluminous granite, radioactivity, Egypt

1. Introduction

Britholite-group minerals are rare silicates (typically P-bearing), with apatite-type structure and the general chemical formula $(REE,Ca)_5[(Si,P)_4]_3(OH,F,Cl)$ with Si > P, where REE usually include yttrium (Pekov et al. 2007). The minerals currently include (with the exception of the tritomite species) six members: (1) britholite-(Ce), (2) britholite-(Y), (3) fluorbritholite-(Ce), (4) fluorbritholite-(Y), (5) fluorcalciobritholite (Pasero et al. 2010), and (6) calciobritholite (Uher et al. 2015). In the literature, the potential phase "alumobritholite" has been reported (Kudrina et al. 1961). Apart from this report, there is no evidence of elevated contents of Al in the minerals of the britholite group. The chemical compositions of britholite-group minerals vary widely, depending on the environment of formation and reflect complex isomorphic substitutions among britholite endmembers (Zozulya et al. 2019). Britholite-(Ce) is more accessible to hydrolysis than the britholite-(Y) (Yunhua, Lipu 1987) and, upon alteration, decomposes or is transformed into other minerals. Britholite minerals may contain high amounts of La, Ce, Nd (Vilalva et al. 2013), and Th (Orlandi et al. 1989), but they are not considered as a traditional ore representing an economically important source for these elements for these elements.

Britholite-group minerals form at the late- to post-magmatic (pegmatite and hydrothermal) stages particularly in alkaline rocks (Arden, Halden 1999; Delta Ventura et al. 1999; Oberti et al. 2001; Vilalva et al. 2013; Zozulya et al. 2019). Their occurrences in

metaluminous types are relatively rare (Macdonald et al. 2013). The author here reports on the unique occurrence of britholite-(Ce) from a metaluminous granite. The granite is part of a 20 km^2 intrusive complex in southwestern Egypt.

2. Site description

The intrusive complex (Fig. 1) crops out in two circular features of ~10 km apart in a sandy plain surrounded by Nubian sandstone that forms the country rocks in the southwestern region of Egypt. It may be linked to the tonalite magma, emplaced in successive phases containing biotite, hornblende or both during the Proterozoic in the region (Sabet 1972; List et al. 1989). The complex of southwestern Egypt is quite different in composition and texture. It comprises four different types of rocks including: (1) granite, (2) granodiorite, (3) tonalite, and (4) monzodiorite (Hassan 2008). These rocks occur in the form of isolated knobs and residual boulders above the Paleozoic-Mesozoic Nubian Formation (Baioumy et al. 2003). The low topographic forms are the remnants of mountains succumbed to desert erosion which is evident from the abundant igneous rock debris and soils in the area. The soil is a fine to medium grained, reddish, thick deposit consisting of quartz, albite, illite, hematite, and trace biotite.

The granite of the studied area consists of quartz and feldspars, with minor amounts of biotite and clinochlore (Hassan 2009). It is enriched in total field gamma (γ)-ray radiation (up to seven orders of magnitude more than the general radiation background), but no obvious mineralization. The primary sources of γ-ray radiation are thorium, uranium, and potassium, specifically ^{232}Th, ^{238}U, and ^{40}K decay chains. Most K is concentrated in the feldspars, while uranium and thorium are incorporated in trace rare-metal phases.

3. Materials and Methods

A hand-held γ-ray counter was used to measure the total gamma ray radiation of the exposed rocks in the field. Two samples of the highly radioactive granite (GR1 and GR2) are used for this research. Polished thin sections were made and studied under plane-polarized (PPL) and cross-polarized transmitted light (XPL) with an Olympus BX41 polarizing microscope. Selected minerals were analyzed using a Hitachi S-4700 Field Emission SEM and Norman Vantage EDS spectrometer at the Institute of Geological Sciences of the Jagiellonian University, Kraków, Poland. The operating conditions were: (1) accelerating voltage 20 kV, (2) beam current 10 nA, (3) counting time 100 seconds, and (4) a beam diameter of < 1 μm. For each analyzed crystal fragment, several points were randomly measured to ensure its homogeneity. The PRZ (Phi-Rho-Z) correction procedure was employed for raw data before normalizing the EDS results. SEM-EDS precision (standard deviation) determined from duplicate mineral spots from the analyzed samples (Table 1) was good for major elements, but it is unacceptable for trace element analyses.

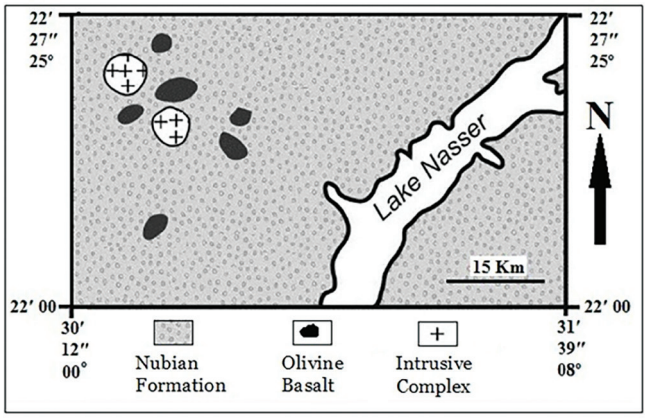

Figure 1. Geological map of southwestern Egypt (modified from EGSMA 1981). The region is a hyperarid desert with maximum daily temperatures ranging from 16°C during December to 48°C in June and rains occurring rarely.

Table 1. SEM-EDS analyses (wt%) of duplicate mineral spots (A and B) from GR1 and GR2; BDL—below detection limit.

	A	B	± 1σ	% Errors
Britholite				
SiO_2	17.10	15.90	0.60	3.64
ThO	7.00	8.34	0.54	8.73
UO_2	BDL	BDL		
ZrO	BDL	BDL		
Al_2O_3	7.90	6.82	0.54	7.34
La_2O_3	13.30	15.10	0.90	6.34
Ce_2O_3	24.70	26.70	1.00	3.89
Pr_2O_3	2.20	1.94	0.13	6.28
Nd_2O_3	5.00	5.15	0.07	1.48
Sm_2O_3	BDL	BDL		
Gd_2O_3	BDL	BDL		
FeO	8.00	7.58	0.21	2.69
Cr_2O_3	BDL	BDL		
MgO	4.30	3.12	0.59	16.0
CaO	5.90	6.50	0.30	4.80
Na_2O	1.24	0.65	0.30	31.22
K_2O	0.53	0.80	0.13	20.30
P_2O_5	BDL	BDL		
SO_3	0.27	0.20	0.03	14.89
F	2.51	1.07	0.72	40.28
Total	99.95	99.87		
Magnetite				
SiO_2	2.40	2.40	0.00	0.00
Al_2O_3	0.60	0.80	0.10	14.28
FeO	93.80	94.70	0.45	0.48
Cr_2O_3	1.14	0.74	0.20	21.28
MgO	0.30	0.40	0.05	14.29
Na_2O	0.70	1.00	0.15	17.65
Total	98.94	100.04		
Zircon				
SiO_2	29.80	28.30	0.75	2.58
ZrO	68.10	67.80	0.15	0.22
Al_2O_3	0.30	0.30	0.00	0.00
FeO	0.70	1.30	0.30	30.00
CaO	0.60	0.30	0.30	33.33
Na_2O	0.50	0.90	0.20	28.57
Total	100.0	98.90		

Whole-rock chemical elements of GR1 and GR2 were analyzed by an inductively coupled plasma-mass spectrometry at Bureau Veritas Commodities Canada Ltd., Vancouver. The accuracy of the analytical results was monitored using reference materials (STD OREAS45E, STD OREAS24P, STD SO-18, STD DOLOMITE-2). In general, the results for these standard materials were within 5-10% of the accepted values.

4. Results and Discussion

4.1. Microscopy and textural analysis

Samples GR1 and GR2 are light grey, fine to medium grained, and exhibit slightly gneissose texture, where felsic layers are thicker than the mafic ones that constitute thin streaks. The samples are composed of oligoclase + K-feldspars + quartz + biotite, the latter is slightly altered to clinochore. The oligoclase occurs as subidiomorphic to xenomorphic crystals that are partially altered to sericite. The K-feldspar is represented by orthoclase and microcline, some of which exhibit perthitic texture and are partially kaolinitized. Quartz was found as strained crystals showing undulose extinction. Small quartz grains are enclosed in larger plagioclase crystals or form myrimkitic intergrowths around plagioclase boundaries. The accessory minerals found in the two studied samples, in decreasing order of abundance, are: britholite-(Ce) > titanite > zircon > magnetite.

Britholite-(Ce) (Fig. 2) typically occurs as independent crystals in the forms of fine-euhedral rhombic prismatic and platy shapes (200-600 µm in size), with straight to suture edges. In plane polarized light, it exhibits a tan pinkish to light brown color; some grains have a darker

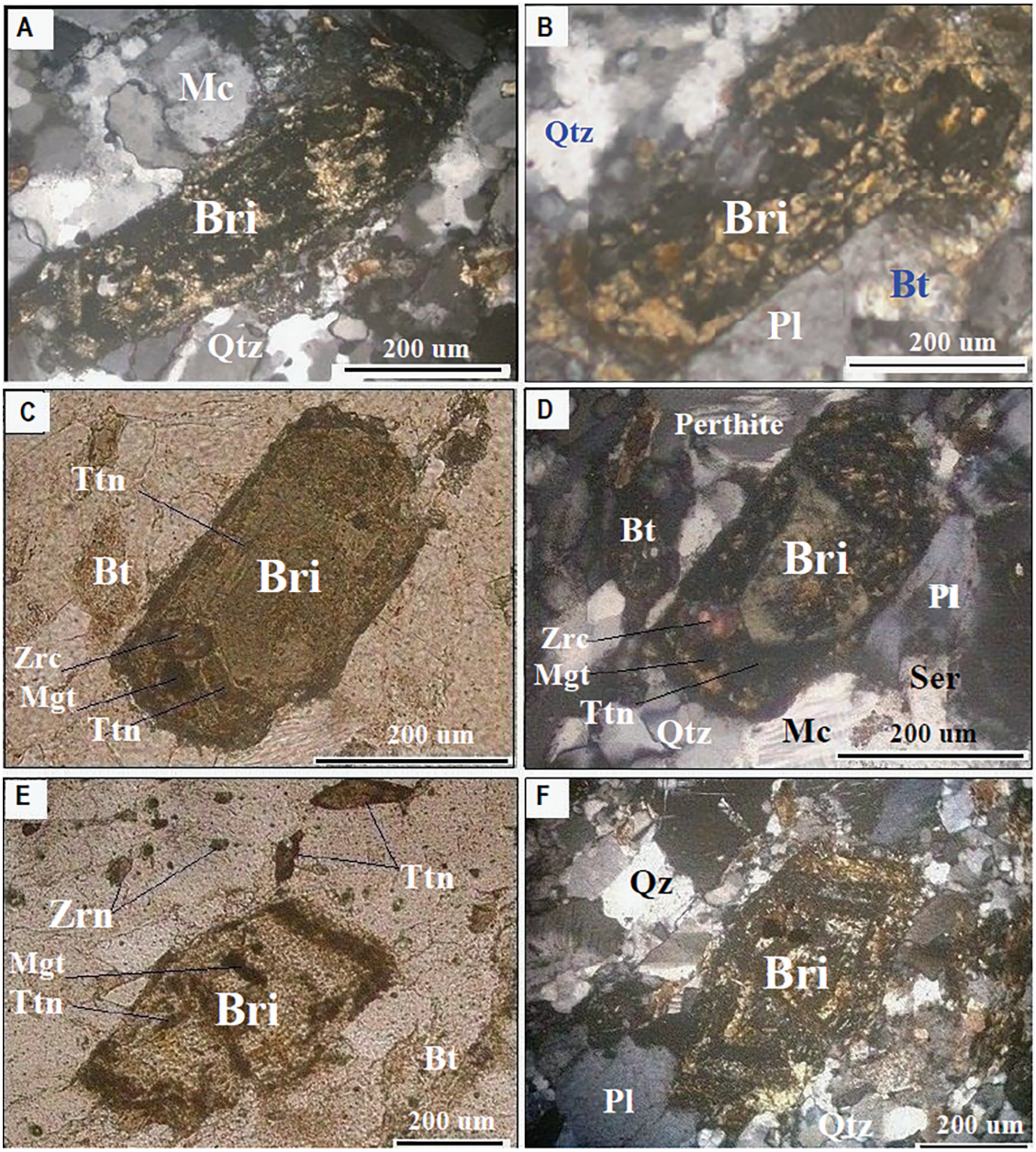

Figure 2. Photomicrographs of samples GR1 and GR2. (A) Image of a britholite prism, taken under XPL. (B) Image of a platy tabular crystal of britholite, taken under XPL. (C-D) Images of a euhedral tabular britholite, taken under PPL and XPL, showing center zonation and a resobed border. (E-F) Images of another euheral britholite, taken under PPL and XPL, showing rims around a core. Mineral abbreviations are: Bt—biotite; Bri—britholite; Mgt—magnetite; Mc—microcline; Pl—plagioclase; Qtz—quartz; Ser—sericite; Zrn—zircon; Ttn—titanite.

orange color. Under cross-polarized light, britholite-(Ce) crystals are heterogeneous and exhibit high relief, dark greenish to brown greenish interference colors. Primary britholite-(Ce) includes magnetite, apatite and zircon and is sometimes included in biotite, leading to the conclusion that it began crystallizing at broadly the same time as biotite, but significantly after feldspars. Several crystals of britholite-(Ce) have slightly concentric zoning and, sometimes, are swelled with spongy texture and resorbed border. The swelling of the crystals indicates that the samples underwent hydration and exchange reactions. Other crystals are intensely fractured, probably due an alteration effect by oxidizing solutions.

Examination of britholite-(Ce) of the samples GR1 and GR2 was made using backscattered electron (BSE) imaging. Typical examples are shown in Figure 3. In BSE images, margins and many parts of the britholite-(Ce) crystals are obscured and, occasionally, are absent, indicating that the crystals are highly altered and decomposed (Fig. 3A,B). Further examination of BSE images reveals that the britholite-(Ce) is made up of smaller grains and fibers with a range of gray shades from white to black (Fig. 3C,D) or it is metamict. Since backscattering increases with increasing atomic number, BSE contrast within a grain is closely related to the distribution of chemical elements (Hall, Lloyd 1981). The change of britholite to another REE phase is seen in BSE images as variations from dark gray to light gray (Fig. 3E,F).

Energy dispersive spectroscopy analyses demonstrate that Ce is predominant over other REE in all of the britholite samples analyzed for this work [Supplementary Electronic Material (SEM) Table S1]. Major elements in the samples (in wt %) are:

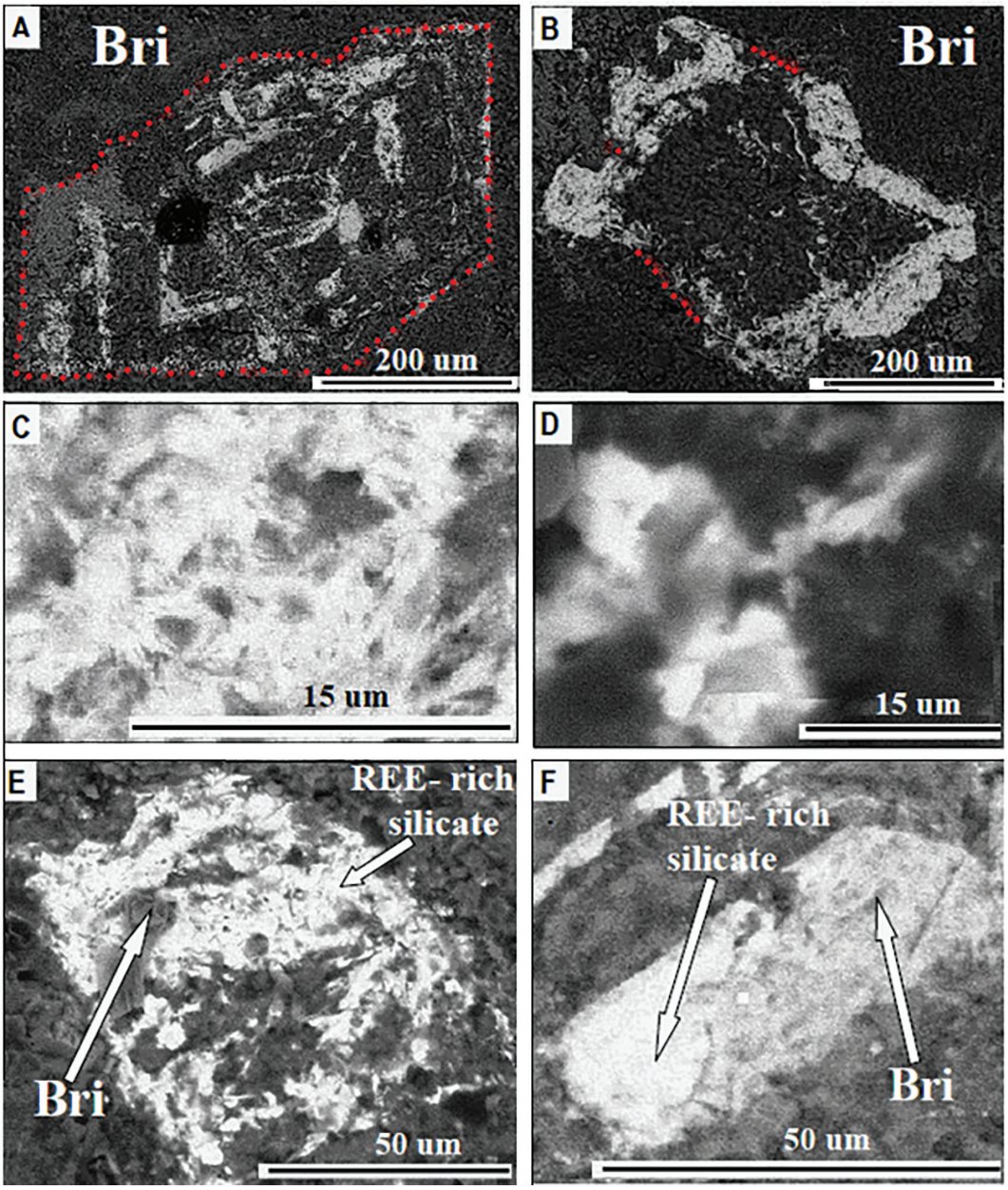

Figure 3. BSE images of REE grains from samples GR1 and GR2. (A) BSE image of the britholite depicted in Fig. 2E, displaying compositional zoning. (B) BSE image of another britholite crystal. In (A) and (B) the dotted red lines partially mark the original crystal outline. (C-D) BSE images of britholite grains with different levels of brightness and, hence, different chemical composition. (E-F) BSE images of britholite partially changed to REE-rich silicate.

$\sum REE_2O$ = 44.8-66.0, Si_2O = 8.9-19.8, CaO = 5.0-13.2, ThO_2 = 4.3-10.1, FeO = 1.1-9.6, Al_2O_3 = 3.0-8.2, MgO = 0.9-5.1, F = 1.2-6.1, Na_2O = 0.6-1.8. The FeO, Al_2O_3, and MgO are generally high compared to reported values for britholite-group minerals from other localities (e.g. Oberti et al. 2001; Pasero et al. 2010; Zozulya et al. 2019). The presence of Fe, Al, and Mg at higher concentions is likely associated with occurrence of microcrystals of clinochlore and/or biotite dispersed within britholite-(Ce) crystals. The britholite-(Ce) analyzed for this study contains significant amounts of Th and U which causes metamictization.

Silica of britholite-(Ce) crystals of samples GR1 and GR2 is negatively correlated with the ΣREE_2O (R^2 = -0.81). As SiO_2 decreases and ΣREE_2O increases the primary magmatic britholite-(Ce) changes to another REE-(Ce) phase. The SiO_2 and Al_2O_3 released during the alteration process form a clay mineral that leached out of the britholite or remains in cracks within the parent mineral. Although the alteration may liberate Th and REE from britholite-(Ce), the presence of fluorine in the oxidizing fluids will prevent the elements from long distance transport and result in their precipitation.

Chemical formulae of britholite-(Ce) (SEM Table S1), calculated on the basis of 13 (O,F,Cl), generally deviate from those expected for typical britholite (T = ~3, M = ~5 apfu, respectively; Pasero et al. 2010). Deviations can be attributed to alteration of samples (as also indicated by petrography and BSE imaging) and/or due to analytical errors. The main composition changes observed in britholite-(Ce) in metalminous granites are due to the following substitutions of Si^{4+} + REE^{3+} for P^{5+} + M^{2+} (Macdonald et al. 2013). The compositions reported in this study and those from literature are evaluated on the basis of these substitutions. The results (Fig. 4A) suggest that the Si^{4+} + substitution mechanism $REE^{3+} \leftrightarrows P^{5+} + M^{2+}$ occur to the extent of 72%. In the britholite series, the incorporation of both U and Th, amongst others, may be accommodated by the substitution mechanism $M^{2+} + (Th^{4+},U^{4+}) \leftrightarrows 2\ REE^{3+}$ (Pan, Flett 2002). The data presented here in Figure 4B suggests that 52% of the variability in the data is controlled by this mechanism.

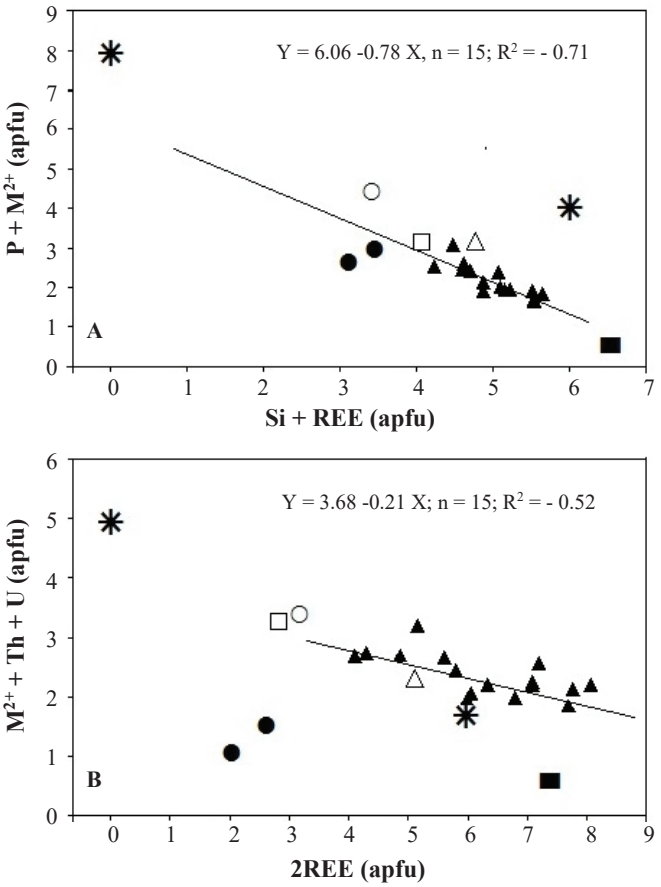

Figure 4. Compositions of the analyzed britholite samples in the cationic diagrams (A) P + M^{2+} versus Si + REE and (B) M^{2+} + Th + U versus 2REE (n = number of samples; R2, coefficient of determination). The ideal apatite and britholite-(Ce) endmembers are plotted as stars. Symbols: filled rectangular, Vilalva et al. 2013; open triangular, Nash 1972; open rectangular, Orlandi et al. 1989; open circular, Mulluso et al. 2012; filled circulars, Kudrina et al. 1961; filled triangular, this work.

4.2. Whole-rock geochemistry

Whole-rock chemical analyses of the granite samples (GR1 and GR2) are given in SEM Table S2, along with the average composition suggested for the upper continental crust (UCC) from Rudnick and Gao (2003). Samples GR1 and GR2 with peralkalinity index (PAI = mol Na_2O + K_2O/Al_2O_3) < 1 and aluminum saturation index (ASI = mol $Al_2O_3/((CaO - (3.33*P_2O_5) + Na_2O + K_2O)$ < 1 are metaluminous. In the IUGS quartz-alkali feldspar-plagioclase diagram of the plutonic rocks, they fall in the monzogranite field (Fig. 5). Both GR1 and GR2 are characterized by elevated Th and U. The concentrations of Th vary between ~51 to 52 ppm and U between ~9 to 10 ppm. The Th and U concentrations are enriched in these samples relative to the UCC by factors of ~5 and 3.5, respectively. Hence, the investigated granite is considered fertile for thorium.

Thorium and uranium are typically covariant under primary magmatic conditions, due to the charge/ionic similarities between the two elements (U^{4+}: 1.05 A˚, Th^{4+}: 1.1 A˚). Consequently, primary igneous rocks vary slightly in Th/U ratios, most of the samples filling in the range 3-4 (Keevil, 1944); thus, GR1 and GR2 with relatively high ratios (5.26-5.64) reflect the retention of thorium and the release of uranium. The fractionation between Th and U can occur at weathering surfaces or due to the effect of hydrothermal (magmatic) fluids where the reduced form of uranium (U^{4+}) oxidized, forming soluble and mobile ion $(U^{6+}O_2)^{2+}$, while Th^{4+} is inoxidizable and, hence, remains behind.

Sample GR1 with total 14 rare earth elements of 297 ppm has a negative Eu anomaly (Eu/Eu* = 0.68; SEM Table S2). Here, the abundance of Eu is depleted relative to the other rare earth elements and this can be taken as evidence for earlier separation of plagioclase. Whole-Rock Eu anomalies are attributed

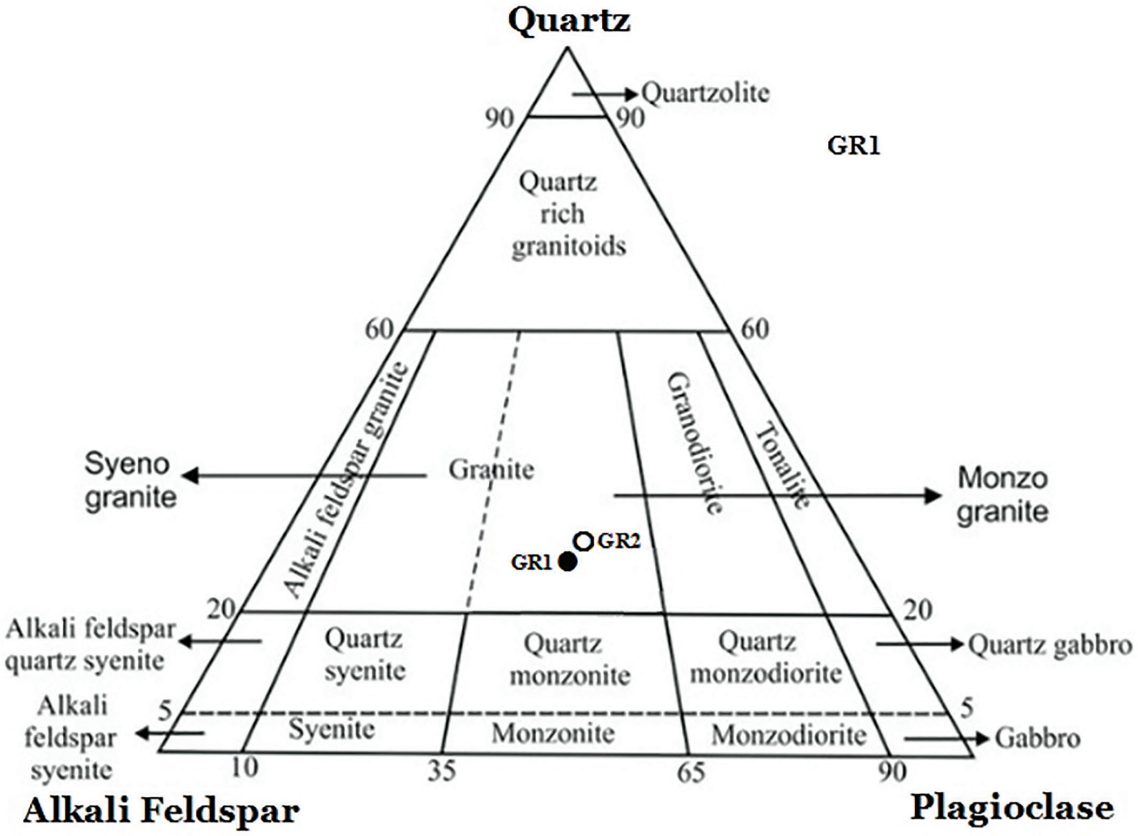

Figure 5. Modal data of the samples GR1 and GR2 plotted on the IUGS quartz-alkaline feldspar-plagioclase diagram of the plutonic rocks.

to the tendency of europium to be incorporated in crystallizing plagioclase, which in turns, is controlled by the chemistry of the melt and reduction-oxidation potential. Europium is incompatible in its trivalent oxidation state (Eu^{3+}—1.07 Å) in an oxidizing magma, but it is preferentially incorporated into crystallizing plagioclase in its divalent form (Eu^{2+}—1.25 Å) in a reducing magma, where it replaces calcium (Ca^{2+}—1.0 Å). Thus, the GR1 with the weakly negative Eu anomaly reflects moderate redox conditions and is typical of upper continental crust rocks (Eu/Eu* = 0.67-0.72, SEM Table S2; Tang et al. 2015).

5. Conclusions

The highly radioactive metalumnious granite of southwestern Egypt, mainly composed of feldspar + quartz + minor biotite + trace clinochlore, contains britholite-(Ce), a light REE-bearing accessory mineral. The britholite-(Ce) occurs as independent prismatic to tabular crystals (< 600 um in size), with considerable amounts of La, Ce, Pr, Nd, and Th. Its crystallization, as suggested from textural features, likely started at approximately the same time as biotite, but significantly after feldspars. Textural and composition data indicate the primary magmatic britholite-(Ce) undergone extensive alteration and chemical modifications.

Acknowledments

The author acknowledges M. Michalik of the Institute of Geological Sciences of the Jagiellonian University, Poland, for SEM-EDX analysis; E.M. Abuzeid of the Nuclear Materials Authority, El Katameya, Egypt for helping with the petrography. Special thanks to the Editor-in-Chief J. Majka and the reviewer A. Włodek whose comments, remarks and suggestions improved this manuscript for publication.

Conflicts of interest

The authors have no conflicts of interest to declare.

Supplementary Material

Supplementary data to this article can be found online at https://doi.org/10.2478/mipo-2023-0002.

References

Arden, K.M., & Halden, N.M. (1999). Crystallization and alteration history of britholite in rare-earth-element-enriched pegmatitic segregations associated with the Eden Lake Complex, Manitoba, Canada. *The Canadian Mineralogist,* 37, 1239–1253. Available from: https://rruff-2.geo.arizona.edu/uploads/CM37_1239.pdf

Baioumy, H.M., Ismael, I.S., & Zidan, I.H. (2003). Clay mineralogy of the Nubia Formation, Western Desert (Egypt). *Geologica Carpathica,* 54, 329–336. Available from: file:///C:/Users/IT%20Computer/Downloads/GeolCarp_Vol54_No5_329_336%20(1).pdf

Della Ventura, G., Williams, C.T., Cabella, R., Oberti, R., Caprilli, E., & Bellatreccia, F. (1999). Britholite-hellandite intergrowths and associated REE-minerals from the alkali-syenitic ejecta of the Vico volcanic complex (Latium, Italy); petrological implications bearing on REE mobility in volcanic systems. *European*

Journal of Mineralogy, 11, 843–854. DOI: 10.1127/ejm/11/5/0843

EGSMA (1981). Geological map of Egypt, scale 1:2,000,000. Geological Survey and Mining Authority, Abbasyia, Cairo, Egypt.

Hall, M.G., & Lloyd, G.E. (1981). The SEM examination of geological samples with a semiconductor back-scattered electron detector. *Americal Mineralogist*, 66, 362-368. https://pubs.geoscienceworld.org/msa/ammin/article-abstract/66/3-4/362/41263/The-SEM-examination-of-geological-samples-with-a?redirectedFrom=fulltext

Hassan, K.M. (2008). Petrography, chemistry and radioactivity of granitoids at north Gebel Seri, South Western Desert, Egypt. *Isotope and Radiation Research,* 40, 615–629. https://inis.iaea.org/search/search.aspx?orig_q=RN:40047318

Hassan, K. M. (2009). Characterization of granites by ^{57}Fe Mössbauer spectroscopy. *Mineralogia,* 40, 95–106. DOI: 10.2478/v10002-009-0008-x

Keevil, B. (1944). Thorium-uranium ratios in rocks and minerals. *American Journal of Science,* 242, 309-321. https://doi.org/10.2475/ajs.242.6.309

Kurdina, M.A., Kurdin, V.S., & Sidorenko, G.A. (1961). Britholite and alumobritholite from alkali pegmatites of Siberia. *Geologiya mestorozhdenii redkikh elementov,* 9, 108–120 (in Russian).

List, F.K., El-Gaby, S., & Tehrani, R. (1989). The basement rocks in the Eastern and Western Deserts and Sinai. In *Stratigraphic lexicon and explanatory note to the geologic map of Egypt 1:500000* (Hermina, M., Klitzsch, E. & List F. eds.). Egyptian General Petroleum Corporation, Cairo, Egypt (33–56).

Macdonald, R., Bagiński, B., Dzierżanowski, P., & Jokubauskas, P. (2013). Apatite-supergroup minerals in UK Palaeogene granites: composition and relationship to host-rock composition. *European Journal of Mineralogy,* 25, 461–471. https://doi.org/10.1127/0935-1221/2013/0025-2291

Melluso, L., De'Gennaro, R., Fedele, L., Franciosi, L., & Morra, V. (2012). Evidence of crystallization in residual, Cl–F-rich, agpaitic, trachyphonolitic magmas and primitive Mg-rich basalt–trachyphonolite interaction in the lava domes of the Phlegrean Fields (Italy). *Geological Magazine*, 149, 532–550. https://doi.org/10.1017/S0016756811000902

Nash, W.P. (1972). Apatite chemistry and phosphorous fugacity in a differentiated igneous intrusion. *American Mineralogist,* 57, 877–886. https://pubs.geoscienceworld.org/msa/ammin/article-abstract/57/5-6/877/542646/Apatite-chemistry-and-phosphorus-fugacity-in-a?redirectedFrom=fulltext

Oberti, R., Ottolino, L., Della Ventura, G., & Parodi, G.C. (2001). On the symmetry and crystal chemistry of britholite: New structural and microanalytical data. *American Mineralogist,* 86, 1066–1075. https://doi.org/10.2138/am-2001-8-913

Orlandi. P., Perchiazzi, N., & Mannucci, G. (1989). First occurrence of britholite-(Ce) in Italy (Monte Somma, Vesuvius). *European Journal of Mineralogy,* 1, 723–725. https://pubs.geoscienceworld.org/eurjmin/article-abstract/1/5/723/61487/First-occurrence-of-britholite-Ce-in-Italy-Monte

Pan. Y., & Fleet, M.E. (2002). Compositions of the apatite-group minerals: Substitution mechanisms and controlling factors. *Reviews in Mineralogy and Geochemistry,* 48, 13–49. https://doi.org/10.2138/rmg.2002.48.2

Paserop, M., Kampf, A.R., Ferraris, C., Pekov, I.V., Rakovan, J., & White, T.J. (2010). Nomenclature of the apatite supergroup minerals. *European Journal of Mineralogy*, 22, 163–179. https://doi.org/10.1127/0935-1221/2010/0022-2022

Pekov, I.V., Pasero, M., Yaskovskaya, A.N., Chukanov, N.V. Puscharovsky, D.Y., Merlino, S., Zubkova, N.V, Kononkova, N.N., Men'shikov, Y.P., & Zadov, A.E. (2007). Fluorcalciobritholite, (Ca, REE)$_5$[(Si, P)O$_4$]$_3$ F, a new mineral: description and crystal chemistry. *European Journal of Mineralogy,* 19, 95–103. https://doi.org/10.1127/0935-1221/2007/0019-0095

Rudnik, R.L. & Gao, S. (2003). Composition of the continental crust. In *Treatise on geochemistry, 3* (Rudnick, R.L., Holland, H.D. & Turekian, K.K. eds.), Elsevier-Pergamon, Oxford (1–64). http://dx.doi.org/10.1016/b0-08-043751-6/03016-4

Sabet, A.H. (1972). On the stratigraphy of basement rocks of Egypt. *Annals of the Geological Survey of Egypt*, II, 79–102.

Tang, M., Rudnick, R.L., Mcdonough, W.F., Gaschnig, R.M., & Huang, Y. (2015). Europium anomalies constrain the mass of recycled lower continental crust. *Geology*, 43, 703–706. https://doi.org/10.1130/G36641.1

Uher, P., Ondrejka, M., Bačík, P., Broska, I., & Konečný, P. (2015). Britholite, monazite, REE carbonates, and calcite: Products of hydrothermal alteration of allanite and apatite in A-type granite from Stupné, Western Carpathians, Slovakia. *Lithos,* 236–237, 212–225. https://doi.org/10.1016/j.lithos.2015.09.005

Vilalva, F.C.J., Vlach, S.R.F., & Simonetti, A. (2013). Nacareniobsite-(Ce) and britholite-(Ce) in peralkaline granites from the Morro Redondo Complex, Graciosa Province, Southern Brazil: occurrence and compositional data. *The Canadian Mineralogist,* 51, 313–332. https://doi.org/10.3749/canmin.51.2.313

Yunhua, S., & Lipu, S. (1987). REE geochemistry of the weathered crust of acid volcanic rocks—an experimental study. *Chinese Journal of Geochemistry,* 6, 165–176. https://link.springer.com/article/10.1007/BF02872217

Zozulya, D., Lyalina, L., Macdonald, R., Bagiński, B., Savchenko, Y., & Jokubauskas, P. (2019). Britholite group minerals from REE-rich lithologies of Keivy alkali granite—Nepheline Syenite Complex, Kola Peninsula, NW Russia. *Minerals,* 9, 732. https://doi.org/10.3390/min9120732

Received: 12 Dec 2022
Accepted: 20 Feb 2023
Handling Editor: Jarosław Majka